

AD_____

Award Number: W81XWH-04-1-0309

TITLE: The Role of TSC1 in the Formation and Maintenance of
Excitatory Synapses

PRINCIPAL INVESTIGATOR: Bernardo L. Sabatini, Ph.D.

CONTRACTING ORGANIZATION: Harvard Medical School
Boston, Massachusetts 02115

REPORT DATE: March 2005

TYPE OF REPORT: Annual

PREPARED FOR: U.S. Army Medical Research and Materiel Command
Fort Detrick, Maryland 21702-5012

DISTRIBUTION STATEMENT: Approved for Public Release;
Distribution Unlimited

The views, opinions and/or findings contained in this report are those of the author(s) and should not be construed as an official Department of the Army position, policy or decision unless so designated by other documentation.

20050826 074

REPORT DOCUMENTATION PAGE

Form Approved
OMB No. 074-0188

Public reporting burden for this collection of information is estimated to average 1 hour per response, including the time for reviewing instructions, searching existing data sources, gathering and maintaining the data needed, and completing and reviewing this collection of information. Send comments regarding this burden estimate or any other aspect of this collection of information, including suggestions for reducing this burden to Washington Headquarters Services, Directorate for Information Operations and Reports, 1215 Jefferson Davis Highway, Suite 1204, Arlington, VA 22202-4302, and to the Office of Management and Budget, Paperwork Reduction Project (0704-0188), Washington, DC 20503

1. AGENCY USE ONLY (Leave blank)		2. REPORT DATE March 2005	3. REPORT TYPE AND DATES COVERED Annual (1 Mar 2004 - 28 Feb 2005)	
4. TITLE AND SUBTITLE The Role of TSC1 in the Formation and Maintenance of Excitatory Synapses			5. FUNDING NUMBERS W81XWH-04-1-0309	
6. AUTHOR(S) Bernardo L. Sabatini, Ph.D.				
7. PERFORMING ORGANIZATION NAME(S) AND ADDRESS(ES) Harvard Medical School Boston, Massachusetts 02115 <i>E-Mail:</i> Bernardo_sabatini@hms.harvard.edu			8. PERFORMING ORGANIZATION REPORT NUMBER	
9. SPONSORING / MONITORING AGENCY NAME(S) AND ADDRESS(ES) U.S. Army Medical Research and Materiel Command Fort Detrick, Maryland 21702-5012			10. SPONSORING / MONITORING AGENCY REPORT NUMBER	
11. SUPPLEMENTARY NOTES				
12a. DISTRIBUTION / AVAILABILITY STATEMENT Approved for Public Release; Distribution Unlimited			12b. DISTRIBUTION CODE	
13. ABSTRACT (Maximum 200 Words) Mutations in the <i>TSC1</i> or <i>TSC2</i> tumor suppressor genes lead to Tuberous Sclerosis Complex, a dominant disorder characterized by benign tumors in multiple organ systems. Patients with TSC also display neurological symptoms including epilepsy, autism, and mental retardation of unclear etiology. We induce loss of <i>Tsc1</i> or <i>Tsc2</i> in a small fraction of differentiated hippocampal pyramidal neurons and demonstrate that the TSC pathway cell-autonomously regulates neuronal structure and function. Loss of <i>Tsc1</i> or <i>Tsc2</i> , including haploinsufficiency of <i>Tsc1</i> , leads to increases in soma size as well as enlargement and loss of dendritic spines. Functional analysis reveals these morphological changes are accompanied by perturbation of electrophysiological properties, including changes in strength and glutamate receptor composition of excitatory synapses. Our results reveal a role for the TSC pathway in the regulation of neuronal structure and function and suggest that cell-autonomous neuronal defects contribute to the pathogenesis of the neurological symptoms of TSC.				
14. SUBJECT TERMS Tuberous sclerosis, synapses, spines, neurons, morphology			15. NUMBER OF PAGES 48	
			16. PRICE CODE	
17. SECURITY CLASSIFICATION OF REPORT Unclassified	18. SECURITY CLASSIFICATION OF THIS PAGE Unclassified	19. SECURITY CLASSIFICATION OF ABSTRACT Unclassified	20. LIMITATION OF ABSTRACT Unlimited	

Table of Contents

Cover.....	1
SF 298.....	2
Table of Contents.....	3
Introduction.....	4
Body.....	4 - 5
Key Research Accomplishments.....	5 - 6
Reportable Outcomes.....	6
Conclusions.....	6
References.....	6
Appendices.....	6

INTRODUCTION

Tuberous Sclerosis (TSC) is an autosomal dominant genetic disorder characterized by benign tumors of many organs. The majority of TSC patients are identified as children and most have neurological symptoms including mental retardation and epilepsy. Although it is known that TSC results from mutations in either the TSC1 or TSC2 genes, the pathogenesis of the neurological disorder is unclear. One possibility, inspired by gross pathological findings, is that the presence of benign growths in the brain leads to disorganized and compressed brain tissue and perturbed neural circuits. However, it is equally possible that loss of TSC1 or TSC2 disrupts neuronal function in a *cell-autonomous* manner. Our hypothesis is that TSC1 is necessary in mature, differentiated neurons for the establishment of proper neuronal morphology and synaptic function. This hypothesis is being tested by examining cell-autonomous defects in TSC1 null neurons located within otherwise normal brain tissue. The approaches used to examine the perturbed cells are immunostaining of activated proteins in the TSC signaling cascade, optical microscopy of neuronal structure, and electrophysiological analysis of electrical properties.

BODY

Task 1. Establish that introduction of Cre recombinase into a TSC1^{C/C} postmitotic neurons results in loss of TSC1 protein.

- a. Prepare dissociated hippocampal cell cultures prepared from TSC1^{C/C} mice*
- b. Assay loss of hamartin in Cre transfected neurons using immunocytochemistry and confocal microscopy*
- c. Determine time course of hamartin loss in neurons*

Tasks 1a and 1b have been completed and the results are shown in Figure 1. Thus we have determined by fluorescence immunohistochemistry (fIHC) that Cre transfected leads to loss of Tsc1 protein. Furthermore, we have shown that the same manipulation leads to increased phosphorylation of the ribosomal protein S6, indicating functional upregulation of the TSC pathway. Task 1c has been partially completed as we have established protein loss within 6 days. However, we have not yet performed other time points to determine if the loss can occur more rapidly or if a longer delay will allow for greater protein loss.

Task 2. Determine if loss of TSC1 leads to perturbed neuronal morphology

- a. Prepare hippocampal slice cultures from TSC1^{C/C} mice*
- b. Sparsely transfect neurons in slice with plasmids encoding Cre and GFP*
- c. Image neuronal morphology at 1, 2, and 3 weeks after transfection*
- d. Perform manual analysis of dendritic morphology and spine length, density, and volume.*
- e. Assay for specificity of effects by determining if transfected with TSC1 rescues any observed alterations of neuronal morphology*

Task 2 a-e has been completed and the results are outlined in Figures 1 and 2. Thus we have performed experiments in organotypic hippocampal slice cultures and demonstrated that Cre transfection (loss of Tsc1) leads to increased soma size, decreased spine density,

and increased spine neck length and head size. These effects are prevented by cotransfection with a plasmid encoding Tsc1, confirming the specificity of the effects. Furthermore, Cre transfection in a separate conditional mouse line (transcriptional stop floxed EGFP in the *Rosa26* locus) does not perturb morphology.

Task 3. Determine if loss of TSC1 perturbs synaptic function.

- a. Prepare hippocampal slice cultures from TSC1^{C/C} mice.*
- b. Sparsely transfect neurons in slice with plasmids encoding Cre and GFP.*
- c. Perform whole-cell electrophysiological analysis of passive neuronal properties (cell capacitance, input resistance, resting membrane potential).*
- d. Perform whole-cell electrophysiological analysis of active neuronal properties (action potential waveform, threshold, and firing rates).*
- e. Perform whole-cell electrophysiological analysis of synaptic function (miniature EPSC rates and amplitude, amplitude of evoked synaptic currents, paired-pulse facilitation, and long-term potentiation)*

Tasks 3a-c have been completed. Task 3d has not started and 3e is approximately 50% complete. The results are summarized in Figure 3. We have shown that, consistent with the increase in cell size, loss of Tsc1 leads to increases in cell capacitance and decreases in input resistance. These changes are accompanied by loss of mEPSCs and increases in the amplitude of AMPA-type glutamate-receptor mediated currents at synapses and increase in AMPA to NMDA receptor currents.

Task 4. Determine if perturbations caused by loss of TSC1 can be rescued by low levels of rapamycin.

- a. Measure pS6 levels in dissociated cultured neurons and determine dose dependence of pS6 on rapamycin levels*
- b. Determine dose of rapamycin that returns pS6 levels in Cre-transfected TSC1^{C/C} neurons to normal levels*
- c. Incubate cultured brain slices in levels of rapamycin normalized pS6 levels and repeat tasks 2-3.*

Preliminary studies have been performed on 4a, b and c. We have used fIHC to measure phosphorylated S6 (pS6) levels in the neuronal soma as in Figure 1. Rapamycin (100 nM) abolishes pS6 staining in both wildtype and Cre-transfected neurons. We have yet to determine a full titration curve of these effects. The effects of rapamycin application on neuronal morphology has been assayed and preliminary results indicate that rapamycin alone leads to increases in spine length. Furthermore, rapamycin is able to return soma size to normal in Tsc1 lacking cells but leads to further perturbations of spine structure. The effects of rapamycin on electrophysiological properties has not been assayed.

KEY RESEARCH ACCOMPLISHMENTS

- Established cell-based, neuronal system for the analysis of morphological and functional perturbations resulting from loss of Tsc1
- Validation of model system, demonstrating that Cre transfection in post-mitotic, differentiated neurons from mice homozygous for conditional Tsc1 alleles leads to loss of Tsc1 and increased pS6.
- Establishment that Tsc1 play2 a role in regulating neuronal morphology and spine structure in differentiated neurons.
- Establishment that these morphological perturbations are accompanied by function changes in passive membrane properties and synaptic transmission.

REPORTABLE OUTCOMES

Manuscript in preparation (attached)

CONCLUSIONS

We have demonstrated that Tsc1 regulates neuronal morphology and function in differentiated, post-mitotic neurons. Loss of Tsc1 leads to changes in cell size (enlarged soma and large spine heads) as well as loss of excitatory synapses (decreased spine density). Furthermore, remaining synapses are functionally perturbed and contain abnormally high levels of AMPA-type glutamate receptors compared to NMDA-type glutamate receptors. Our results indicate that functional perturbations of neurons may contribute to the pathogenesis of TSC. In addition, our experiments with rapamycin suggest that its application is unable to reverse morphological defects resulting from Tsc1 loss and thus may not have therapeutic value in the treatment of the neurological symptoms of TSC.

REFERENCES Manuscript attached -submitted for publication

APPENDICES Manuscript attached (same as above)

**Regulation of neuronal morphology and function by the tumor suppressors
Tsc1 and Tsc2**

Sohail F. Tavazoie^{1*}, Veronica A. Alvarez^{1*}, Dennis A. Ridenour¹, David J.
Kwiatkowski², Bernardo L. Sabatini¹

1. Department of Neurobiology
Harvard Medical School
220 Longwood Ave
Boston, MA 02115

2. Department of Medicine
Brigham and Women's Hospital
Harvard Medical School
221 Longwood Ave,
Boston MA 02115

* indicates equal contribution

Running title: Tsc1/2 regulate neuronal morphology and function

Acknowledgements:

We thank members of the Sabatini lab, Dietmar Schmucker and David Sabatini for comments on the manuscript and Susan Dymecki, Elizabeth Henske, Vijaya Ramesh, Lewis Cantley and Yang Shi for the gifts of reagents. This work was supported by a Burroughs Wellcome Fund Career Award and McKnight Technological Innovations Grant (to BLS), and the Department of Defense (TS030004). The authors declare that they have no financial conflicts of interests.

DRAFT

Submitted for publication

Mutations in the *TSC1* or *TSC2* tumor suppressor genes lead to Tuberous Sclerosis Complex (TSC), an autosomal dominant disorder characterized pathologically by benign tumors in multiple organ systems. Patients with TSC also display neurological symptoms including epilepsy, autism, and mental retardation of unclear etiology. Here we induce loss of Tsc1 or Tsc2 in a small fraction of post-mitotic, differentiated hippocampal pyramidal neurons and demonstrate that the TSC pathway regulates neuronal structure and function in a cell-autonomous manner. Loss of Tsc1 or Tsc2, including haploinsufficiency of Tsc1, leads to increases in soma size as well as enlargement and loss of dendritic spines. Functional analysis reveals that morphological changes triggered by loss of Tsc1 are accompanied by perturbation of electrophysiological properties, including changes in the strength and glutamate receptor composition of excitatory synapses. Our results reveal a role for the TSC pathway in the regulation of neuronal structure and function and suggest that cell-autonomous neuronal defects contribute to the pathogenesis of the neurological symptoms of TSC.

TSC1 and *TSC2* are tumor suppressor genes whose protein products, hamartin (TSC1) and tuberin (TSC2), negatively regulate cell growth in a variety of systems. In humans, heterozygous mutations in either *TSC1* or *TSC2* lead to Tuberous Sclerosis Complex, an autosomal dominant hamartomatous disorder characterized by benign tumors in multiple organs including the brain, kidneys, heart, and eyes [1]. TSC also

typically presents with a constellation of neurological deficits that include epilepsy, mental retardation, and autism.

Biochemical and genetic analyses in mammalian systems and *Drosophila* have revealed that TSC1 and TSC2 participate in a conserved growth-regulating pathway involving the mammalian target of rapamycin (mTOR) [2-5]. In brief, the activation of growth-promoting receptor tyrosine kinases, such as the insulin receptor, stimulates phosphoinositide 3-kinase (PI3K) and the serine/threonine kinase Akt (also referred to as protein kinase B or PkB) (reviewed in [6]). In vitro, Akt is able to phosphorylate TSC2 at conserved consensus phosphorylation sequences and downregulate its GTPase activated protein (GAP) activity [7-9]. Reduced TSC2 GAP activity allows the buildup of the GTP-bound form of the small GTPase Rheb [10] [11] and upregulates mTOR, which, through multiple actions, enhances protein translation and cell growth [6]. Thus, given the loss of heterozygosity of *TSC1* or *TSC2* found in hamartomas of TSC patients [12], the growth of these benign tumors is thought to result from the increased mTOR activity and uncontrolled cell growth that accompanies interruption of the TSC pathway.

The pathogenesis of the neurological symptoms of TSC is unclear and loss of heterozygosity is not seen within the brain of TSC patients [13]. The function of the TSC pathway in post-mitotic mammalian neurons has not been identified and what defects arise from haploinsufficiency of TSC1 or TSC2 are unknown. However, many parallels exist between the TSC pathway and those that link extracellular stimuli to synaptic refinement in neurons. For example, activation of the TrkB receptor tyrosine kinase by brain-derived neurotrophic factor (BDNF) stimulates PI3K and Akt to promote dendritic growth [14] and synaptic refinement [15]. BDNF also triggers long-term potentiation of

synaptic strength (BDNF-LTP) through a mechanism that is blocked by rapamycin, a potent and specific inhibitor of mTOR [16]. Similarly, strong activation of metabotropic glutamate receptors depresses synaptic transmission through a PI3K and mTOR-dependent pathway [17] [18] [19]. These forms of synaptic plasticity are thought to require protein translation within dendrites and mTOR and its downstream signaling partners, including p70S6K and 4EBP1, are found at or near synapses [20-22]. Thus, the TSC pathway is likely to regulate synaptic structure and function.

Here we examine the role of the TSC pathway in controlling growth of post-mitotic, differentiated neurons, focusing particularly on the regulation of specialized cellular protuberances called dendritic spines. These structures consist of a bulbous spine head separated from the parent dendrite by a thin neck and, in the mammalian brain, each spine head typically houses one and only one synapse (reviewed in [23]). Growth of dendritic spines is intimately tied to development and regulation of excitatory synapses. In the developing brain, dendritic spines appear during periods of synaptogenesis and the maturation of synapses is accompanied by a morphological progression from elongated spines with small heads to shorter spines with larger heads. In established neuronal circuits, patterns of synaptic activity that induce potentiation of synaptic connections trigger the appearance of new spines and the enlargement of pre-existing spines whereas those stimuli that depress synaptic transmission have opposite effects [24, 25] [26].

By analyzing the structure and function of neurons in genetically mosaic brain tissue, we demonstrate that the TSC pathway cell-autonomously regulates the number and size of dendritic spines as well as the properties of excitatory synapses. These effects do not require regulation of Tsc2 by Akt at conserved phosphorylation sites and are

mediated by rapamycin-sensitive mTOR signaling as well as by rapamycin-independent pathways. Furthermore, the TSC pathway is sensitive to gene-dosage effects, such that loss of a single copy of *Tsc1*, as is present in all neurons of TSC patients, is sufficient to perturb dendritic spine structure. Our results demonstrate that the TSC pathway regulates neuronal structure and function and suggest that intrinsic perturbations of neuronal function are likely to contribute to the etiology of the neurological symptoms of Tuberous Sclerosis Complex.

Results

In order to examine defects in neuronal structure and function caused by perturbation of the TSC pathway, we exploited an existing transgenic mouse carrying a conditional allele of *Tsc1* (*Tsc1^C*) in which exons 17 and 18 of the gene are flanked by loxP sequences [27]. Loss of Tsc1 protein in neurons following transfection with a plasmid encoding a Cre recombinase-nuclear localization sequence fusion protein (Cre) was confirmed in dissociated hippocampal cultures prepared from mice homozygous for the conditional allele (*Tsc1^{C/C}*). Since transfection efficiency of post-mitotic, differentiated neurons is low, Tsc1 protein levels were monitored by performing immunocytochemistry for Tsc1 and measuring fluorescence levels in the cytoplasm of individual neurons (Fig. 1a,b). Neurons were identified by expression of MAP-2 in dendrites and transfection was judged by the presence of strong immunostaining for Cre in the nucleus (Fig. 1a). In neurons expressing Cre, cytoplasmic Tsc1 immunofluorescence levels were significantly reduced at 6 days post transfection (DPT) compared to untransfected neighboring neurons (Fig. 1b).

In a variety of cell types, down-regulation of TSC1 or TSC2 upregulates mTOR activity and increases phosphorylation of the ribosomal protein S6 [3, 5, 9]. However, little is known about the regulation of S6 in mammalian neurons. Immunostaining against phosphorylated S6 (pS6) revealed a perinuclear cytoplasmic signal in neurons (Fig. 1c) that was abolished by application of rapamycin, a selective pharmacological inhibitor of mTOR (data not shown). pS6 levels were substantially higher in the cytoplasm of Cre-transfected *Tsc1^{C/C}* neurons than in neighboring control neurons (Figs. 1c,d). Thus, Cre transfection in post-mitotic, differentiated *Tsc1^{C/C}* neurons induces

recombination of the *Tsc1^C* allele and loss of Tsc1 protein. Furthermore, reduced Tsc1 levels lead to increased pS6 staining, indicating that Tsc1 normally represses the phosphorylation of ribosomal protein S6 in neurons.

Tsc1 and Tsc2 regulate cell growth in differentiated pyramidal neurons

Widespread loss of Tsc1 in the mouse brain, even when limited to astrocytes, leads to pronounced seizures and early death [27]. Seizure activity triggers secondary changes in gene expression and synapse structure and function that may obscure cell-autonomous neuronal defects caused directly by loss of Tsc1. To avoid these complications we generated genetically mosaic brain tissue in which a small number of neurons lacking Tsc1 were located in otherwise genetically normal brain tissue. This was accomplished by sparse biolistic transfection of pyramidal neurons with Cre recombinase and GFP in organotypic hippocampal brain slices prepared from *Tsc1^{C/C}* mice. In this preparation, the majority of cells express Tsc1 and thus most of the synaptic partners of neurons lacking Tsc1 are wildtype. Furthermore, by triggering loss of Tsc1 in post-mitotic, differentiated neurons, developmental and cell migration defects are avoided.

Transfected pyramidal hippocampal neurons were readily identifiable by their characteristic morphology when imaged using two-photon laser scanning microscopy (2PLSM) (Fig. 1e) and by the location of their somas in a cell-dense band (Fig. 3d). Somas of pyramidal neurons with Cre-induced loss of Tsc1 were larger than those of control neurons (Figs. 1e-g). Soma size was dramatically increased at 20 DPT with mean soma reaching ~2 fold control levels. Changes in soma size were prevented by cotransfection with a plasmid encoding Tsc1, confirming that the increase was due to loss

of *Tsc1* and not to expression of Cre recombinase. Furthermore, application of rapamycin (100 nM) during the time interval 14-20 DPT reversed the increase in soma size, indicating that rapamycin-sensitive mTOR activity is epistatic to *Tsc1* with respect to the control of neuronal soma size.

To further control for nonspecific effects of Cre-mediated DNA recombination, similar measurements were made in tissue prepared from B6;129-*Gt(ROSA)26Sor^{tm2Sho}*/J mice that carry a floxed transcriptional stop upstream of the EGFP coding sequence in the *Rosa26* locus (*Rosa^{C/C}*). Cre expression in *Rosa^{C/C}* neurons had no effects on soma size (Fig. 1g).

Similar measurements of soma size were carried out in rat neurons in which loss of *Tsc2* was induced by RNA-interference (Fig 1g, see methods). Transfection of dissociated rat hippocampal pyramidal neurons with a dual-promoter plasmid encoding CMV-driven GFP and a U6-driven short-hairpin RNA targeting *Tsc2* (shTsc2) resulted in loss of *Tsc2* immunostaining and upregulation of pS6 levels (Sup Figure 1). In organotypic hippocampal slices, at 10 DPT, somas of pyramidal neurons transfected with shTsc2 were greatly enlarged relative to those of control neurons. A summary of the soma sizes for each genotype and pharmacological condition is given in Supplemental Table 1. This effect was occluded by application of rapamycin or by cotransfection with human TSC2, which contains 9 base pair changes within the region targeted by shTsc2 (Fig. 1g).

Tsc1 and Tsc2 regulate spine size

In pyramidal neurons, the vast majority of excitatory synapses are made onto the heads of dendritic spines, and the morphology and density of dendritic spines reflect the properties and number of synapses. At 20 DPT, dendritic spines of *Tsc1^{C/C}* neurons expressing GFP alone, used as controls, displayed roughly spherical spine heads separated from the dendrite by thin necks (Fig. 2a). In contrast, apical and basal dendrites of *Tsc1^{C/C}* neurons expressing Cre and GFP possessed elongated spines with greatly enlarged, bulbous heads. Quantification of these changes showed that Tsc1 loss increased spine length and spine head width as well as decreased the density of dendritic spines compared to control (Figs. 2b, c). Similar effects on spine size and morphology are seen at 10 DPT (Fig 2), a time point at which loss of Tsc1 has no effect on soma size (Fig. 1g). Changes in spine morphology and density were prevented by expression of *Tsc1* (Fig. 2b, c) and no changes in spine density or morphology were seen with Cre expression in *Rosa^{C/C}* neurons (Supplemental table 1), confirming that the morphological changes seen with Cre expression in *Tsc1^{C/C}* neurons were due to loss of Tsc1 protein.

The perturbations of spine morphology triggered by loss of Tsc1 are phenocopied by RNAi mediated knock-down of Tsc2 in rat hippocampal neurons (Fig. 2c, 4d). Thus, at both 10 and 20 DPT, dendritic spines of shTsc2 expressing neurons are elongated with enlarged spine heads. These effects were rescued by expression of hTsc2 (Fig. 2c). Summaries of the average spine densities, lengths, and head widths for each genotype and pharmacological condition are given in Supplemental Table 1.

Functional defects associated with loss of Tsc1

Do the enlarged spine heads seen following loss of Tsc1 contain functionally perturbed synapses? To address this question, whole-cell voltage-clamp recordings were performed from *Tsc1^{CC}* pyramidal neurons transfected with Cre and untransfected neighboring neurons (Fig. 3a). A red fluorophore was included in the recording pipette solution in order to fill the neuron and confirm its identity and recordings of spontaneous miniature excitatory postsynaptic currents (mEPSCs) were made. The frequency of mEPSC reflects the number of functional synapses containing AMPA-type glutamate receptors (AMPA) whereas the amplitude of mEPSCs is determined by the number of AMPAR at the postsynaptic density. At 10 DPT, the amplitude of mEPSCs was increased by ~ 20% (Fig. 3b,c) in Cre-expressing neurons compared to neighboring control neurons, indicating an enhanced sensitivity to released neurotransmitter likely due to an increased number of postsynaptic AMPAR. No changes in mEPSC frequency (Fig. 3c, right panel) or in passive membrane properties such as the resting membrane resistance (R_{in}) and cell capacitance (C_m) were seen (in controls: $R_{in} = 197 \pm 43 \text{ M}\Omega$, $C_m = 256 \pm 61 \text{ pF}$; in Cre neurons: $R_{in} = 200 \pm 63 \text{ M}\Omega$, $C_m = 182 \pm 34 \text{ pF}$). At 20 DPT, resting membrane resistance of cells lacking Tsc1 was greatly reduced from $185 \pm 20 \text{ M}\Omega$ in control neurons to $127 \pm 15 \text{ M}\Omega$ in Cre-expressing cells ($n=13$ cells in each condition, $P < 0.05$), making the comparison of mEPSCs between Tsc1-lacking neurons and control neurons impossible ($C_m = 171 \pm 17 \text{ pF}$ for controls and $234 \pm 24 \text{ pF}$ for Cre neurons). The reduced input resistance and increased membrane capacitance are expected from the enlarged surface area of Tsc1-lacking neurons.

At 20 DPT, evoked EPSCs were monitored in CA1 pyramidal neurons following stimulation of Schaffer collaterals. For these experiments, axons making synapses onto transfected or control neurons were stimulated with a bipolar electrode placed in the stratum radiatum (Fig. 3d). The synaptic responses were monitored at a holding potential of -60 mV, at which only AMPARs are activated, and at $+40$ mV, at which the block of NMDA-type glutamate receptors (NMDAR) by magnesium is relieved and the long-lived NMDAR component of the EPSC is revealed (Fig 3e). Increases in the ratio of evoked AMPAR to NMDAR current amplitudes is seen during normal development as well as following stimulation paradigms that trigger long-term potentiation (LTP) of synaptic responses. In Cre-transfected neurons, the AMPAR/NMDAR current ratio was significantly increased to 3.7 ± 0.71 from 2.0 ± 0.35 in controls, indicating a developmentally aberrant increase in levels of synaptic AMPAR.

To assess possible changes in presynaptic function induced retrogradely by postsynaptic loss of Tsc1, responses to a pair of stimuli were recorded and paired-pulse facilitation (PPF) was measured. PPF is a synaptic parameter determined by presynaptic release probability and was calculated as the ratio of the amplitude of the second synaptic current to that of the first. PPF was found to be similar in untransfected and Cre-transfected neurons (PPF= 1.73 ± 0.22 in control and 1.75 ± 0.15 in Cre neurons) (Fig. 3g), indicating a lack of retrograde modulation of presynaptic function and confirming that the synaptic defects result from altered function of the postsynaptic neuron. Thus, loss of Tsc1 results in synapses with higher numbers of AMPAR that displayed increased sensitivity to glutamate and increased AMPAR/NMDAR current ratios.

Neuronal morphology is sensitive to haploinsufficiency of Tsc1

Individuals afflicted with TSC carry heterozygous mutations in either the *TSC1* or *TSC2* genes and loss of heterozygosity, unlike in hamartomas, is not seen within the brain. Thus, complete loss of TSC1 or TSC2 function is not necessary for the development of neurological symptoms. Therefore we asked if loss of a single copy of *Tsc1* is sufficient to trigger changes in neuronal morphology (Fig. 4a, b). In tissue prepared from *Tsc1*^{C/+} mice, expression of Cre led to increases in soma size compared to GFP-transfected neurons. Similarly, *Tsc1*^{C/+} Cre-expressing neurons had decreased spine density, increased spine length, and increased spine head width relative to *Tsc1*^{C/+} GFP-expressing neurons (Figs. 4b). For all measured parameters, the morphological changes were less pronounced for loss of a single copy than for loss of both copies of *Tsc1*, suggesting that the TSC pathway is sensitive to gene dosage.

The TSC pathway regulates spine morphology through rapamycin-sensitive and insensitive pathways

Rapamycin is a potent and specific inhibitor of mTOR, and is predicted to act downstream of TSC1 and TSC2. In order to examine if the effects of loss of *Tsc1* or *Tsc2* on neuronal morphology are mediated by increased rapamycin-sensitive activity of mTOR, we examined the ability of rapamycin to reverse defects in neuronal morphology. Neurons in hippocampal organotypic slices were transfected and maintained in culture for 14 days, a time point at which the effects of Cre-mediated loss of *Tsc1* and RNAi-mediated loss of *Tsc2* were apparent (Figs. 1, 2). Rapamycin (100 nM) was then added

to the culture media, and the cultures were maintained for 6 more days before analysis (total of 20 DPT).

Application of rapamycin to GFP-expressing rat pyramidal neurons induced the growth of long, thin spines (Fig. 4c,5b). Surprisingly, the length of dendritic spines in the presence of rapamycin was found to be substantially longer than those of control neurons and even longer than those of Tsc2 knockdown cells (Fig. 4c-d, Summary data in Fig. 5b). This suggests a role for mTOR in the normal regulation of spine morphology. The rapamycin-induced spine phenotype was clearly distinguishable from that resulting from loss of Tsc2, as rapamycin treated neurons lacked enlarged spine heads. Application of rapamycin to Tsc2 knockdown cells triggered the growth of exceedingly long processes with small spine heads (Fig. 4d, 5b). Similarly, in Cre-expressing *Tsc1^{C/C}* neurons, rapamycin reversed the enlargement of spine heads but led to a further increase in spine length (Supplemental table 1).

Epistatic analysis of Tsc2 and Akt

Akt has been proposed to inhibit TSC by phosphorylation at two sites (S939 and T1462, numbered by the human sequence) conserved in *Drosophila* and mammals [8]. However, the role of regulation of TSC2 by Akt in the control of cell growth in vivo is controversial. In HEK293 cells, human TSC2 (hTSC2) with these amino acids mutated to alanine (TSC2^{S939A/T1462A} referred to as hTSC2^{AA}) reduces serum-induced activation of S6-kinase without affecting other Akt substrates [8]. Similarly, deletions of or mutations in homologous sites in *Drosophila* Tsc2 (dTsc2^{S924A/T1518A}) repress the increase in ommatidia size associated with enhanced Akt expression [7]. However, dTsc2^{S924A/T1518A} is

able to fully rescue the lethality of dTsc2 null phenotype in *Drosophila*, indicating that regulation by Akt at these sites is not required for normal fruit fly development [28].

We asked whether Akt regulates neuronal morphology in our system through phosphorylation of S939 and T1462 of Tsc2. Expression in rat hippocampal pyramidal neurons of a constitutively active Akt (Akt CA), consisting of a myristoylated Akt lacking its pleckstrin homology domain (myrAkt Δ 4-129) [29], resulted in large somas, long spines and increased spine head size (Fig. 5). Thus, upregulation of Akt phenocopies loss of Tsc1/Tsc2.

Three experiments were performed to determine if these effects are mediated by downregulation of Tsc2 by Akt through phosphorylation of S939 and T1462 (Fig. 5 and Supplemental Table 1). First, hTSC2^{AA} was expressed alone and found to have no effect on spine or somatic morphology. Second, expression of hTSC2^{AA} failed to occlude the enlargement of somas and spines triggered by overexpression of Akt CA. Third, hTSC2^{AA} was expressed in Tsc2 knockdown cells and found to rescue spine and soma morphological changes triggered by shTsc2 with efficiency equal to that of wildtype hTSC2. Thus, our data indicate that phosphorylation of S939 and T1462 is not necessary for regulation of neuronal soma and spine size by Tsc2, and that hTSC2^{AA} is unable to act as a dominant negative with respect to the increases in cell size triggered by upregulated Akt activity.

Discussion

We show that loss of Tsc1 or Tsc2 in hippocampal pyramidal neurons results in increases in the size of somas and dendritic spines, as well as a decrease in spine density. Whole-cell recordings indicate that these enlarged spines house stronger synapses that are more sensitive to glutamate as a consequence of elevated numbers of AMPA-type glutamate receptors. Thus, downregulation of Tsc1 or Tsc2 promotes mature spine morphology (large spine heads) via an mTOR-dependent mechanism as well as mature receptor composition in the synapse (high AMPA/NMDA current ratio). Conversely, repression of mTOR with rapamycin promotes the maintenance of the immature spine phenotype (long spines with small or unidentifiable spine heads). Thus, our results are consistent with the TSC pathway normally controlling synaptic maturation through regulation of mTOR.

Relationship of Tsc2 and Akt

We find that expression of constitutively active Akt phenocopies the morphological defects seen with loss of Tsc1 or Tsc2. Increased Akt activity leads to enlarged neuronal size, in agreement with similar studies using overexpression of Akt or downregulation of PTEN, the lipid phosphatase that antagonizes PI3K [7, 30-33]. However, we find that the somatic and dendritic spine enlargement induced by increased Akt activity is independent of phosphorylation of TSC2 at S939 and T1462, the strong consensus sites conserved across *Drosophila*, rats, mice, and humans. This is in contrast to findings in *Drosophila* in which enlargement of ommatidia triggered by overexpression of Akt is prevented by expression of dTsc2^{S924A/T1518A} [7]. Furthermore, we find that

expression of hTSC2^{AA} does not perturb spine and soma size and that it reverts the effects of loss of endogenous Tsc2. Again these results are in contrast with the dramatic reduction in ommatidia size following dTsc2^{S924A/T1518A} expression [7] but in agreement with recent findings that dTsc2^{S924A/T1518A} is able to rescue the dTsc2-null phenotype in *Drosophila* development [28]. In summary, our data indicate that, although upregulation of Akt and downregulation of Tsc1/2 result in similar phenotypes, phosphorylation of Tsc2 at S939 and T1462 is not necessary for the normal control of neuronal size or for the neuronal enlargement induced by upregulation of Akt.

mTOR-dependent and independent effects of loss of Tsc1/2

Are the effects of TSC1 or TSC2 loss on neuronal morphology mediated exclusively by mTOR or do these proteins regulate morphology via independent pathways? Both TSC1 and TSC2 are reported to participate in mTOR-independent signaling cascades that may regulate cell morphology. TSC1 interacts with and regulates the cytoskeleton via a C-terminal domain that binds ezrin-radixin-moesin (ERM) family proteins and an N-terminal domain capable of activating Rho GTPase in human endothelial cells [34]. TSC2 has been shown to activate Rho (in MDCK and ELT3 cells) [34] and increased Rho activity in hippocampal pyramidal neurons decreases spine length [35]. Furthermore, Rho GDP/GTP exchange factors (Rho-GEF) regulate dendritic spine morphology and density [36, 37]. TSC2 also interacts with 14-3-3 proteins [38, 39], whose many cellular functions include trafficking of ion channels from the endoplasmic reticulum [40] and regulation of the actin cytoskeleton [41]. Importantly, TSC1 and TSC2 proteins stabilize each other [42], and thus reduced expression of either protein

may induce a common set of morphological perturbations mediated through disruption of these mTOR-independent signaling cascades.

Our data indicate that the effects of Tsc1 or Tsc2 loss are mediated by both mTOR-dependent and -independent pathways. Application of rapamycin to neurons with reduced Tsc1 or Tsc2 levels restores neuronal soma size to control levels, indicating that mTOR is epistatic to Tsc1/2. On the other hand, in the presence of rapamycin, spine morphology is clearly different in control neurons than in neurons with reduced Tsc1/2, arguing against a strictly epistatic relationship. These differential effects of rapamycin can be seen graphically by plotting, for each genotype and pharmacological condition, the changes in spine density, length, and head half-width against the change in soma size (Fig 6a). The degree to which spine density, spine head width, and soma size are perturbed by manipulations of the TSC pathway covary tightly (Fig. 6a), suggesting that these effects depend on common downstream mediators. Furthermore, in the presence of rapamycin (Fig. 6b), the changes in spine head half-width are predicted by the effects on soma size using the same linear relationship found in the absence of rapamycin. In contrast, in the presence of rapamycin, spine length is increased beyond the expected level. Our findings suggest that Tsc1/2 regulate soma and spine size via an rapamycin-sensitive mTOR-dependent pathway and spine length via a rapamycin-insensitive pathway.

Implication for Tuberous Sclerosis Complex

Patients with TSC exhibit perturbations of cortical architecture including tubers, disorganized regions of the brain with disturbed lamination containing increased numbers of astrocytes and sparse neurons [1]. Correlation between the number of cortical tubers

and the severity of seizure symptoms has led to the notion that the neurological deficits in TSC arise from disruptions of cortical architecture [43]. Here we show that loss of a single copy of *Tsc1* results in clear defects in neuronal morphology, including increased soma size, decreased spine density and increased spine size. Therefore we propose that cell-autonomous neuronal defects triggered by haploinsufficiency of *TSC1* or *TSC2*, in addition to the perturbations of brain architecture caused by cortical tubers, subependymal nodules, and giant cell astrocytomas, contribute to the pathogenesis of the neurological symptoms of TSC.

Rapamycin, as a highly specific antagonist of mTOR, is currently in clinical trial as a therapeutic agent for the treatment of renal angiomyolipomas in TSC patients. Will antagonizing the action of mTOR have therapeutic value for the treatment of neurological symptoms of TSC patients? We find that the morphological perturbations triggered by loss of *Tsc1* or *Tsc2* are due to rapamycin sensitive and insensitive signaling cascades and that rapamycin is unable to rescue the *Tsc1/2* loss phenotype. Thus, rapamycin is unlikely to fully reverse the neurological symptoms of TSC and, given the reported sensitivity of various forms of synaptic plasticity to rapamycin, may cause further cognitive deficits.

Experimental Procedures

Animals

Mice carrying a conditional *Tsc1* allele (*Tsc1^C*) consisting of LoxP elements upstream of exon 17 and downstream of exon 18 were used in this study [27]. *Tsc1^{C/+}* mice were generated by crossing *Tsc1^{C/C}* mice with wildtype C57Bl6 mice (Charles River Laboratories, MA). *Rosa^{C/C}* mice were purchased from Jackson laboratory. This strain contains the Enhanced Green Fluorescent Protein (EGFP) coding sequence with an upstream LoxP-flanked stop fragment inserted into the Gt(ROSA)26Sor locus. Male and female Sprague-Dawley rats were purchased from Charles River Laboratory. All animal procedures were conducted following Harvard Medical School guidelines.

Tsc1^C genotyping was performed using mouse tail genomic DNA and primers F4536 (5'-ACGAGGCCTCTTCTGCTACC-3') and R4830 (5'-CAGCTCCGACCATGAAGT-3'). PCR conditions consisted of 35 cycles of 92° for 30 seconds, 55° for 30 seconds, and 72° for 1 minute yielding a 295 and 480 bp products from the wild-type and conditional alleles, respectively.

Plasmids

All enzymes were obtained from New England Biolabs (Beverly, MA). The following plasmids were gifts: pBS:: β -actin-nls-Cre (Susan Dymecki, Harvard Medical School, Boston, MA); hTSC2 and hTSC2^{AA} (Aristotelis Astrinidis and Elisabeth Henske, Philadelphia, PA); pBS/U6 (Yang Shi, Harvard Medical School). pEGFP-N1 (Invitrogen, Carlsbad, CA) was used as GFP control. For construction of the dual

promoter CMV-EGFP/U6-shRNA vector, pEGFP-N1 was digested with BamHI and BglII to remove the multiple cloning site (MCS) and religated to create pEGFP-N1::ΔMCS. The U6 promoter and its downstream MCS from pBS/U6 were then inserted into pEGFP-N1::ΔMCS at the filled-in AflII site downstream of the SV40 polyadenylation sequence in either the forward (pGUF) or reverse (pGUR) orientation relative to EGFP. Four sets of shRNAs directed against Tsc2 were designed by searching Tsc2 for sequences that were 19-21 base pairs in length, conserved in mice and rats, and had a G:C content around 50%. These were used to construct oligos containing the target sequence, a restriction site, the reverse complement of the target sequence, 5 T's for U6 polymerase termination, and an EcoRI site for cloning. All oligos were ordered from IDT (Coralville, IA). shTsc2 Clone 4-1 was used in this study and was constructed from oligos:

oligos: Tsc2-4F
 (GGTGAAGAGAGCCGTATCACAAAGCTTTGTGATACGGCTCTCTTCACCCTTT
 TTG) and Tsc2-4R

(AATTCAAAAAGGGTGAAGAGAGCCGTATCACAAAGCTTTGTGATACGGCTC
 TCTTCACC). For production of shTsc2, pGUF was digested with ApaI, Klenowed, digested with EcoRI, and treated with calf intestinal alkaline phosphatase (CIP). Tsc2-4R and 4F were annealed, phosphorylated with T4 polynucleotide kinase, and ligated into the digested pGUF to yield shTsc2. Use of this dual promoter vector guarantees that GFP expressing cells also express the hairpin RNA.

For construction of the Cre reporter construct, pHcLoxGFP, oligos were ordered containing 5' restriction sites, LoxP sequences and the 20 base pairs of either the 5' end of HcRed (from pHcRed1-N1, Clontech, Palo Alto, CA) or the 3' end of SV40

polyadenylation sequence. The PCR amplified, floxed HcRed1-SV40pA fragment was cloned into the EcoRI and BamHI sites of pEGFP-N1.

Cell culture and transfection

Dissociated hippocampal cultures were prepared from postnatal day 3 Sprague-Dawley rats and mice, as previously described [44]. Cells were plated at a density of 8×10^4 cells/well on confluent glial monolayers on 12-mm glass coverslips. Cultures were transfected with Lipofectamine 2000 (Invitrogen) after 3-5 days of culture in neuronal NEU media lacking biotin and following manufacture guidelines [44].

Hippocampal slices were prepared from mouse and rat brains as previously described [45]. This preparation preserves the three-dimensional architecture and local environment of neurons and glia to a much greater degree than dissociated neuron cultures. Slices were prepared from P5-P7 pups and biolistically transfected with a Helios Gene Gun (Biorad) after 2 days in culture, typically resulting in approximately 10 transfected neurons per slice. Bullets were prepared using 12.5 mg of 1.6 μ m gold particles and 40-80 μ g of plasmid DNA. Cotransfection of Cre and GFP was confirmed using the Cre reporter construct pHcLoxGFP. Neurons transfected with this construct alone display red fluorescence. In neurons cotransfected with pHcLoxGFP and Cre recombinase, HcRed is excised and expression of GFP is activated. The shift from red to green fluorescence in neurons transfected with bullets containing both Cre and pHcLoxGFP was evaluated in more than a dozen organotypic slices. At 24 hours, both

red and green cells were visualized. After 48 hours, however, only green cells were seen, suggesting efficient Cre-mediated recombination and a high rate of plasmid co-transfection.

Immunofluorescence

Dissociated hippocampal neurons were fixed on coverslips with PBS solution containing 3.7% paraformaldehyde/4% sucrose. Cells were permeabilized with 0.1% Triton for 10', blocked in 1% goat serum (Jackson ImmunoLabs) and incubated with the following primary antibodies: anti-Phospho-S6 Ribosomal Protein (1:100, Ser 235/236; Cell Signaling), anti-MAP-2 (1:500, IgG₁; Sigma), anti-MAP-2 (1:500, Chemicon), anti-CRE recombinase (1:1000, IgG_{1k}; Chemicon), anti-CRE recombinase (1:1000, Novagen). The following antibodies were kindly provided by S. Han and V. Ramesh (Massachusetts General Hospital): anti-Tuberin (TS; affinity-eluted polyclonal), anti-Hamartin (1B2A8; monoclonal), anti-Hamartin (HF6; affinity-eluted polyclonal). The following secondary antibodies from Jackson ImmunoResearch were used at a dilution of 1:500: Cy3-conjugated goat anti-rabbit IgG (H+L), Cy3-conjugated goat anti-mouse IgG (H+L), Cy5-conjugated goat anti-rabbit IgG (H+L), and Cy5-conjugated Goat anti-mouse IgG (H+L). Confocal images were obtained on an LSM510 (Zeiss).

2-Photon laser scanning microscopy

2PLSM was performed using custom built microscopes constructed around a commercial fluorescence microscope (BX51WI, Olympus) as described previously [46, 47]. A Ti:sapphire laser (Mira, Coherent) pumped by a 10 W laser (Verdi, Coherent) was

tuned to 910 nm. The laser output was 3X expanded, modulated with Pockels cells (350-50 Conoptics) and gated by a mechanical shutter (Uniblitz, Vincent Associates). The scanning mirrors (HP6810, Cambridge Technology) were focused onto the back focal plane of the objective (60X, NA 0.9, Olympus) by a scan lens (Olympus) and a tube lens (CVI laser). Fluorescence was detected with photomultiplier tubes (PMTs) (R3895, Hamamatsu) through the objective and a 1.4 NA oil condenser in epifluorescence and transfluorescence modes, respectively. Laser-scanning differential interference contrast was implemented with the addition of a partially reflective cover slip and photodiode in the transfluorescence path. Two PMTs were used in each of the epifluorescence and transfluorescence pathways for "green" and "red" fluorescence detection and signals combined at the input of a transimpedance amplifier (SR570, Stanford Research Systems). Appropriate dichroics (565 dclpxr, Chroma) and filters (607/45LP, BG22, Chroma) were used to spectrally separate red and green emitted photons. Image acquisition and analysis was performed using ScanImage [48].

Image acquisition and analysis

Slice cultures were placed in the imaging chamber and submerged in ACSF. Transfected pyramidal neurons throughout the CA fields of hippocampus were identified based on their green fluorescence, characteristic morphology, and presence in a cell-body dense layer. Low power images of pyramidal neurons were acquired at 0.8x zoom (image field= 300x270 μ m) whereas spiny regions of basal and apical dendrites were imaged with 5x zoom (image field= 42x42 μ m). Optical sections were an average of two scans

and were 1.0 μm apart. Spine density, length and half-width, as well as soma size were determined manually using custom software [49] written in MATLAB (Mathworks, Natick MA). All experiments were analyzed blind to genotype. Spine lengths were measured from the tip of the protrusion to the junction with the dendritic shaft. No attempt was made to distinguish filopodia from spines. Spine head width was measured by determining the fluorescence distribution in a line across the thickest portion of the spine head and was calculated by examining the width of the distribution where fluorescent intensity fell to 30% of its maximal value. Similar measurements performed on 100 nm diameter yellow-green fluorescent microspheres (FluorSpheres[®], Molecular Probes, Eugene, OR) indicated that the point spread function of our microscope placed a lower limit on measurable half-widths of 550 nm. Since the apparent spine head width is given by the convolution of the true fluorescence distribution and point-spread function of the microscope, the apparent head width is the sum of the true head width and 550 nm. Thus, we have displayed the summaries of spine head widths (Fig. 2b,5b) from this lower bound and have subtracted this value in the determination of relative changes in spine head width for the summary presented in Figure 6. Soma cross sectional area was measured in the maximum intensity projection of a low-power image stack of the soma by manually drawing an outline around the soma and counting the number of pixels contained within it.

Electrophysiology

Hippocampal slice cultures were placed in the recording chamber of a 2PLSM perfused with artificial cerebrospinal fluid (ACSF) containing (in mM): 127 NaCl, 25

NaHCO₃, 1.25 Na₂HPO₄, 2.5 KCl, 2 CaCl₂, 1 MgCl₂, 25 glucose and saturated with 95% O₂, 5% CO₂ at room temperature. Whole-cell voltage-clamp recordings were performed from Cre-transfected pyramidal neurons (green fluorescence and visible gold particle in soma) and control untransfected neighbors at 10-12 and 18-20 days post-transfection. Unlike for the morphological analyses, untransfected neighboring neurons were used as control in the electrophysiological studies because they represent an internal control for the viability of the slice culture, the degree of spontaneous activity, the relative position of the stimulation electrode and the strength of stimulation. GFP-transfected neurons were indistinguishable from untransfected neurons with regards to their membrane properties, ruling out electrophysiological changes due to GFP expression (data not shown).

Pipettes were pulled from borosilicate glass capillary tubing with filaments to yield tips of 3-5 MΩ resistance and filled with internal solution containing (in mM): 120 cesium methane-sulfonate, 10 HEPES, 10 EGTA, 4 MgCl₂, 0.4 NaGTP, 4 MgATP, 10 phosphocreatine, 0.02 Alexa Fluor-594, pH= 7.3 (290 mOsm). Bicuculline (20 μM) was added to the bath to block GABA_A receptors in all experiments and tetrodotoxin (1 μM) was included to block sodium channels for the recordings of mEPSCs. Recordings were made using an Axopatch 200B amplifier (Axon Instruments, Union City, CA), filtered at 2kHz and digitized at 10kHz. Series resistance (8-19 MΩ), input resistance and membrane capacitance were calculated from a 5 mV, 50 ms hyperpolarizing step. Series resistance was monitored online and recordings were discontinued if it increased over 20 MΩ. Analyses of mEPSC frequency and amplitude were performed in Igor Pro

(Wavemetrics, Lake Oswego, OR) using custom software that identified events based on rise time and amplitude thresholds.

For the recording of evoked EPSCs, a bipolar stimulating electrode was placed in the stratum radiatum at 250-350 μm from the soma of the recorded neuron and stimuli were delivered at 0.125 Hz. Cells were voltage-clamped at -60 mV and +40 mV for the measurements of AMPA and NMDA components of the EPSCs, respectively. Paired stimuli with an interpulse interval of 50 ms were delivered while holding the cells at -60 mV. Ten to thirty trials were averaged per cell at each holding potential and the peak amplitude and the late component of EPSCs (100 ms from the peak) were measured to determine the AMPAR/NMDAR current ratio. Paired pulse facilitation (PPF) was calculated as the ratio between the peak amplitude of the second EPSC and the first.

Statistics

Unless otherwise stated, statistical significance was judged by ANOVA with, when appropriate, a Tukey-Kramer correction for multiple pairwise comparisons in Matlab or Microsoft Excel. The distributions of mEPSC amplitudes and fluorescent immunostaining intensities were compared using the nonparametric Kolmogorov-Smirnov test.

Figure Legends

Figure 1 Cre expression in hippocampal neurons of *Tsc1^{C/C}* mice leads to loss of Tsc1 protein, increased phosphorylation of S6, and increased soma size. **(a)** Image of untransfected (top) and Cre-transfected (bottom) neurons in a dissociated hippocampal culture from *Tsc1^{C/C}* mice with immunoreactivity to MAP2 and Cre shown in red and to Tsc1 in green. Arrow highlights red nucleus indicative of expression of the Cre-NLS fusion protein. **(b)** Cumulative distribution of Tsc1 immunostaining in Cre-transfected (black) and untransfected (red) neurons at 6 DPT. Fluorescence levels from the secondary antibody were measured in cytoplasm of Cre-transfected and untransfected neurons ($P < 0.05$ by Kolmogorov-Smirnov test). **(c)** Image of untransfected (top) and Cre-transfected (bottom) neurons with immunoreactivity to MAP2 and Cre shown in red and to pS6 in green. Arrow highlights red nucleus indicative of expression of the Cre-NLS fusion protein. **(d)** Cumulative distribution of pS6 immunostaining in Cre-transfected (black) and untransfected (red) neurons at 6 DPT ($P < 0.05$ by Kolmogorov-Smirnov test). **(e)** 2PLSM images of GFP-transfected (left) and GFP/Cre cotransfected (right) pyramidal neurons in organotypic hippocampal slice cultures prepared from *Tsc1^{C/C}* mice. **(f)** Enlarged views of the somas from the neurons shown in panel e. **(g)** Summary of effects of loss of Tsc1 or Tsc2 on cross-sectional area of somas of hippocampal pyramidal neurons. The effects of Tsc1 loss at 20 DPT are suppressed by cotransfection with Tsc1 or treatment with rapamycin. Expression of Cre in neurons from mice homozygous for a conditional-stop GFP in the ROSA26 locus (*Rosa^{C/C}*) has no effect on soma size. The effects of Tsc2 knockdown at 10 DPT are suppressed by

cotransfection with human Tsc2 or upon treatment with rapamycin.* = $p < 0.05$ compared to control. # = $p < 0.05$ compared to Cre-transfected neurons.

Figure 2 Loss of Tsc1 leads to increased size but decreased density of dendritic spines.

(a) Images of apical (left) and basal (right) dendrites from *Tsc1^{C/C}* pyramidal neurons in hippocampal organotypic slice culture. Neurons were transfected with GFP alone (top) or GFP and Cre (bottom). (b) Cumulative distribution of spine length and head width from *Tsc1^{C/C}* neurons transfected with GFP alone (red), GFP and Cre (black), or GFP, Cre, and Tsc1 (thick black line) at 20 DPT. (c) Summary of effects of Tsc1 or Tsc2 loss on dendritic spine density, length and head width. * = $P < 0.05$ compared to control neurons. # = $P < 0.05$ for rescue experiments compared to perturbed phenotype (Cre or shTsc2 expressing cells as appropriate).

Figure 3 Loss of Tsc1 leads to an increase in synaptic AMPA-type glutamate receptors.

(a) *left*, Laser-scanning DIC image of the pyramidal cell layer of an organotypic slice culture from a *Tsc1^{C/C}* mouse with superimposed fluorescence image of a GFP expressing neuron. Note the gold particle (arrow) in the nucleus of the transfected neuron. Image of a Cre/GFP-transfected pyramidal neuron before (middle) and after (right) filling a red fluorophore through a whole-cell recording electrode. (b) Representative traces of mEPSCs recorded from control and Cre-transfected *Tsc1^{C/C}* neurons. Scale bars: 20pA, 200ms. (c) Cumulative distribution of mEPSC amplitude for control (gray line) and Cre-transfected (black line) *Tsc1^{C/C}* neurons recorded at 10 DPT (left) (n=660 and 781 mEPSCs from 10 and 12 cells, respectively). Amplitude distributions in Cre neurons

were different than control ($P < 0.05$, Kolmogorov-Smirnov test). Frequency of mEPSCs (mean and standard error) for untransfected (gray) and Cre-transfected (black) *Tsc1*^{C/C} pyramidal neurons at 10 DPT (right). (d) Wide-field image of a hippocampal organotypic slice culture from a *Tsc1*^{C/C} mouse showing sparse GFP transfection of neurons in the pyramidal cell layer (pcl) and a schematic of relative positions of the recording electrode (rec) and stimulating electrode (stim) within the slice. (e) Evoked EPSCs recorded at -60mV (negative current) and +40mV (positive current) with arrowheads showing the times at which AMPAR (negative) and NMDAR (positive) mediated currents were measured (left). Mean AMPAR/NMDAR current ratios for control (gray bar) and Cre-transfected (black bar) *Tsc1*^{C/C} neurons at 20 DPT (n=11 and 13 cells, respectively; * = $P < 0.05$) (right). (f) Example trace of paired-pulse facilitation measured at a 50 ms interpulse interval in a Cre-transfected *Tsc1*^{C/C} neuron at 20 DPT and summary data for control (gray bar) and Cre-transfected (black bar) neurons.

Figure 4 Neuronal morphology is sensitive to haploinsufficiency of *Tsc1* and suppression of mTOR activity. (a) Images of dendrites of Cre/GFP (left) and GFP (right) transfected pyramidal neurons in hippocampal organotypic slice cultures prepared from *Tsc1*^{C/+} mice at 20 DPT. (b) Relative soma cross-sectional area, spine density, length, and head width for Cre-transfected *Tsc1*^{C/+} (gray bars) and *Tsc1*^{C/C} (black bars) neurons compared to GFP-transfected neurons of each genotype. * = $P < 0.05$. (c and d) Images of GFP (c) and shTSC2 (d) transfected pyramidal neurons in organotypic slice cultures of rat hippocampus at 20 DPT. Low-power images of the whole cell (left) and enlarged views of spiny dendrites (right) are shown. Representative images are shown for cells

incubated in control media for 20 DPT (top) or for 14 days in control media followed by 6 days in 100 nM rapamycin (bottom).

Figure 5 Akt upregulation phenocopies Tsc1/Tsc2 loss but does not require phosphorylation of Tsc2 at conserved Akt phosphorylation sites. **(a)** Images of pyramidal neurons (left) in organotypic slice cultures of rat hippocampus and enlarged views of spiny dendrites (right). Neurons were transfected with an Akt CA (top); Akt CA and hTSC2^{AA} (middle); or shTsc2 and hTSC2^{AA} (bottom) and imaged at 10 DPT **(b)** Summary of effects of Akt upregulation, Tsc2 knockdown, hTSC2^{AA} expression, and mTOR blockade with rapamycin on spine density, length, and head width. * = $P < 0.05$ compared to control neurons. # = $P < 0.05$ for rescue experiments compared perturbed phenotype (shTsc2 or Akt CA expressing neurons, as appropriate).

Figure 6 Tsc1 and Tsc2 regulate neuronal morphology by mTOR-dependent and independent mechanisms. **(a)** Relative changes in spine density, length, and head width plotted as a function of relative changes in soma area. Data are shown for Cre-expressing *Tsc1*^{C/+} neurons (filled triangles); Cre-expressing *Tsc1*^{C/C} neurons at 10 and 20 DPT and following rescue with Tsc1 (filled squares); and shTsc2-expressing rat neurons at 10 and 20 DPT and following rescue with hTSC2 (open squares). Data from GFP-transfected neurons in each genotype define the 100% control level for each parameter (gray diamond). Linear regression (lines) shows a strong anticorrelation of the effects on spine density and soma size and strong positive correlation of effects on spine head width and soma size ($P < 0.05$ for each). Regression coefficients for each linear fit are shown.

(b) Relative changes in spine density, length, and head width plotted as a function of changes in soma size measured in the presence of rapamycin for Cre-expressing *Tsc1^{Cre}* neurons (filled squares), shTsc2-expressing rat neurons (open squares), and GFP-transfected rat neurons (gray diamond). Data are shown overlaid on the linear regressions (solid lines) and their 95% confidence bands (dashed, curved lines) calculated from the data in (a). (c) Schematic of the effects of loss of Tsc1/2 or incubation in rapamycin on soma size, spine length, and spine head size. The effects on soma size and spine head width are mTOR-dependent whereas those on spine length occur through an unknown, mTOR-independent pathway.

Supplemental Figure 1. Knock-down of Tsc2 by RNA-interference

Cumulative distribution of Tsc2 immunofluorescence in shTSC2-transfected (black) and shGFP control (red) neurons at 6 DPT (left). Cumulative distribution of pS6 immunostaining in shTSC2-transfected (black) and shGFP control (red) neurons at 6 DPT (right).

References

1. Gomez, M., S. JR, and H.W. V, eds. *Tuberous Sclerosis Complex*. 3 ed. 1999, Oxford University Press.
2. Ito, N. and G.M. Rubin, *gigas, a Drosophila homolog of tuberous sclerosis gene product-2, regulates the cell cycle*. *Cell*, 1999. **96**(4): p. 529-39.
3. Potter, C.J., H. Huang, and T. Xu, *Drosophila Tsc1 functions with Tsc2 to antagonize insulin signaling in regulating cell growth, cell proliferation, and organ size*. *Cell*, 2001. **105**(3): p. 357-68.
4. Tapon, N., et al., *The Drosophila tuberous sclerosis complex gene homologs restrict cell growth and cell proliferation*. *Cell*, 2001. **105**(3): p. 345-55.
5. Gao, X. and D. Pan, *TSC1 and TSC2 tumor suppressors antagonize insulin signaling in cell growth*. *Genes Dev*, 2001. **15**(11): p. 1383-92.
6. Hay, N. and N. Sonenberg, *Upstream and downstream of mTOR*. *Genes Dev*, 2004. **18**(16): p. 1926-45.
7. Potter, C.J., L.G. Pedraza, and T. Xu, *Akt regulates growth by directly phosphorylating Tsc2*. *Nat Cell Biol*, 2002. **4**(9): p. 658-65.
8. Manning, B.D., et al., *Identification of the tuberous sclerosis complex-2 tumor suppressor gene product tuberin as a target of the phosphoinositide 3-kinase/akt pathway*. *Mol Cell*, 2002. **10**(1): p. 151-62.
9. Inoki, K., et al., *TSC2 is phosphorylated and inhibited by Akt and suppresses mTOR signalling*. *Nat Cell Biol*, 2002. **4**(9): p. 648-57.
10. Stocker, H., et al., *Rheb is an essential regulator of S6K in controlling cell growth in Drosophila*. *Nat Cell Biol*, 2003. **5**(6): p. 559-65.
11. Garami, A., et al., *Insulin activation of Rheb, a mediator of mTOR/S6K/4E-BP signaling, is inhibited by TSC1 and 2*. *Mol Cell*, 2003. **11**(6): p. 1457-66.
12. Sepp, T., J.R. Yates, and A.J. Green, *Loss of heterozygosity in tuberous sclerosis hamartomas*. *J Med Genet*, 1996. **33**(11): p. 962-4.
13. Ramesh, V., *Aspects of tuberous sclerosis complex (TSC) protein function in the brain*. *Biochem Soc Trans*, 2003. **31**(Pt 3): p. 579-83.
14. Dijkhuizen, P.A. and A. Ghosh, *BDNF regulates primary dendrite formation in cortical neurons via the PI3-kinase and MAP kinase signaling pathways*. *J Neurobiol*, 2005. **62**(2): p. 278-88.
15. Mizuno, M., et al., *Phosphatidylinositol 3-kinase: a molecule mediating BDNF-dependent spatial memory formation*. *Mol Psychiatry*, 2003. **8**(2): p. 217-24.
16. Tang, S.J., et al., *A rapamycin-sensitive signaling pathway contributes to long-term synaptic plasticity in the hippocampus*. *Proc Natl Acad Sci U S A*, 2002. **99**(1): p. 467-72.
17. Hou, L. and E. Klann, *Activation of the phosphoinositide 3-kinase-Akt-mammalian target of rapamycin signaling pathway is required for metabotropic glutamate receptor-dependent long-term depression*. *J Neurosci*, 2004. **24**(28): p. 6352-61.
18. Zhou, Q., K.J. Homma, and M.M. Poo, *Shrinkage of dendritic spines associated with long-term depression of hippocampal synapses*. *Neuron*, 2004. **44**(5): p. 749-57.

19. Huber, K.M., M.S. Kayser, and M.F. Bear, *Role for rapid dendritic protein synthesis in hippocampal mGluR-dependent long-term depression*. *Science*, 2000. **288**(5469): p. 1254-7.
20. Asaki, C., et al., *Localization of translational components at the ultramicroscopic level at postsynaptic sites of the rat brain*. *Brain Res*, 2003. **972**(1-2): p. 168-76.
21. Burnett, P.E., et al., *Neurabin is a synaptic protein linking p70 S6 kinase and the neuronal cytoskeleton*. *Proc Natl Acad Sci U S A*, 1998. **95**(14): p. 8351-6.
22. Sabatini, D.M., et al., *Interaction of RAFT1 with gephyrin required for rapamycin-sensitive signaling*. *Science*, 1999. **284**(5417): p. 1161-4.
23. Nimchinsky, E.A., B.L. Sabatini, and K. Svoboda, *Structure and function of dendritic spines*. *Annu Rev Physiol*, 2002. **64**: p. 313-53.
24. Toni, N., et al., *LTP promotes formation of multiple spine synapses between a single axon terminal and a dendrite*. *Nature*, 1999. **402**(6760): p. 421-5.
25. Maletic-Savatic, M., R. Malinow, and K. Svoboda, *Rapid dendritic morphogenesis in CA1 hippocampal dendrites induced by synaptic activity*. *Science*, 1999. **283**(5409): p. 1923-7.
26. Matsuzaki, M., et al., *Structural basis of long-term potentiation in single dendritic spines*. *Nature*, 2004. **429**(6993): p. 761-6.
27. Uhlmann, E.J., et al., *Astrocyte-specific TSC1 conditional knockout mice exhibit abnormal neuronal organization and seizures*. *Ann Neurol*, 2002. **52**(3): p. 285-96.
28. Dong, J. and D. Pan, *Tsc2 is not a critical target of Akt during normal Drosophila development*. *Genes Dev*, 2004. **18**(20): p. 2479-84.
29. Kohn, A.D., et al., *Construction and characterization of a conditionally active version of the serine/threonine kinase Akt*. *J Biol Chem*, 1998. **273**(19): p. 11937-43.
30. Tuttle, R.L., et al., *Regulation of pancreatic beta-cell growth and survival by the serine/threonine protein kinase Akt1/PKBalpha*. *Nat Med*, 2001. **7**(10): p. 1133-7.
31. Verdu, J., et al., *Cell-autonomous regulation of cell and organ growth in Drosophila by Akt/PKB*. *Nat Cell Biol*, 1999. **1**(8): p. 500-6.
32. Kwon, C.H., et al., *Pten regulates neuronal soma size: a mouse model of Lhermitte-Duclos disease*. *Nat Genet*, 2001. **29**(4): p. 404-11.
33. Backman, S.A., et al., *Deletion of Pten in mouse brain causes seizures, ataxia and defects in soma size resembling Lhermitte-Duclos disease*. *Nat Genet*, 2001. **29**(4): p. 396-403.
34. Lamb, R.F., et al., *The TSC1 tumour suppressor hamartin regulates cell adhesion through ERM proteins and the GTPase Rho*. *Nat Cell Biol*, 2000. **2**(5): p. 281-7.
35. Govek, E.E., et al., *The X-linked mental retardation protein oligophrenin-1 is required for dendritic spine morphogenesis*. *Nat Neurosci*, 2004. **7**(4): p. 364-72.
36. Penzes, P., et al., *The neuronal Rho-GEF Kalirin-7 interacts with PDZ domain-containing proteins and regulates dendritic morphogenesis*. *Neuron*, 2001. **29**(1): p. 229-42.
37. Penzes, P., et al., *Rapid induction of dendritic spine morphogenesis by trans-synaptic ephrinB-EphB receptor activation of the Rho-GEF kalirin*. *Neuron*, 2003. **37**(2): p. 263-74.

38. Li, Y., et al., *Regulation of TSC2 by 14-3-3 binding*. J Biol Chem, 2002. **277**(47): p. 44593-6.
39. Hengstschlager, M., et al., *Tuberous sclerosis genes regulate cellular 14-3-3 protein levels*. Biochem Biophys Res Commun, 2003. **312**(3): p. 676-83.
40. Nufer, O. and H.P. Hauri, *ER export: call 14-3-3*. Curr Biol, 2003. **13**(10): p. R391-3.
41. Gohla, A. and G.M. Bokoch, *14-3-3 regulates actin dynamics by stabilizing phosphorylated cofilin*. Curr Biol, 2002. **12**(19): p. 1704-10.
42. Benvenuto, G., et al., *The tuberous sclerosis-1 (TSC1) gene product hamartin suppresses cell growth and augments the expression of the TSC2 product tuberin by inhibiting its ubiquitination*. Oncogene, 2000. **19**(54): p. 6306-16.
43. Shepherd, C.W., O.W. Houser, and M.R. Gomez, *MR findings in tuberous sclerosis complex and correlation with seizure development and mental impairment*. AJNR Am J Neuroradiol, 1995. **16**(1): p. 149-55.
44. Boyer, C., T. Schikorski, and C.F. Stevens, *Comparison of hippocampal dendritic spines in culture and in brain*. J Neurosci, 1998. **18**(14): p. 5294-300.
45. Stoppini, L., P.A. Buchs, and D.A. Muller, *A simple method for organotypic cultures of nervous tissue*. J. Neurosci. Methods, 1991. **37**: p. 173-182.
46. Carter, A.G. and B.L. Sabatini, *State-dependent calcium signaling in dendritic spines of striatal medium spiny neurons*. Neuron, 2004. **44**(3): p. 483-93.
47. Yasuda, R., B.L. Sabatini, and K. Svoboda, *Plasticity of calcium channels in dendritic spines*. Nat Neurosci, 2003. **6**(9): p. 948-55.
48. Pologruto, T.A., B.L. Sabatini, and K. Svoboda, *ScanImage: flexible software for operating laser scanning microscopes*. Biomed Eng Online, 2003. **2**(1): p. 13.
49. Trachtenberg, J.T., et al., *Long-term in vivo imaging of experience-dependent synaptic plasticity in adult cortex*. Nature, 2002. **420**(6917): p. 788-94.

Figure 2

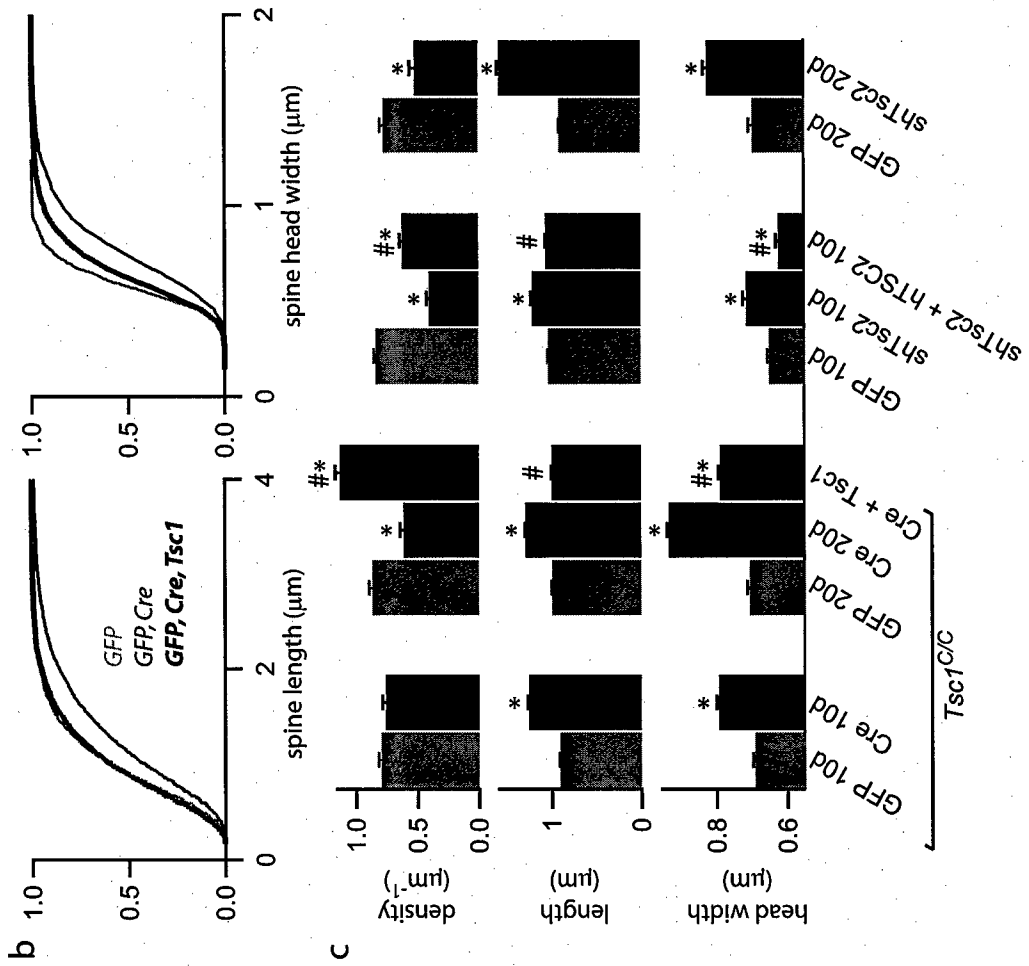
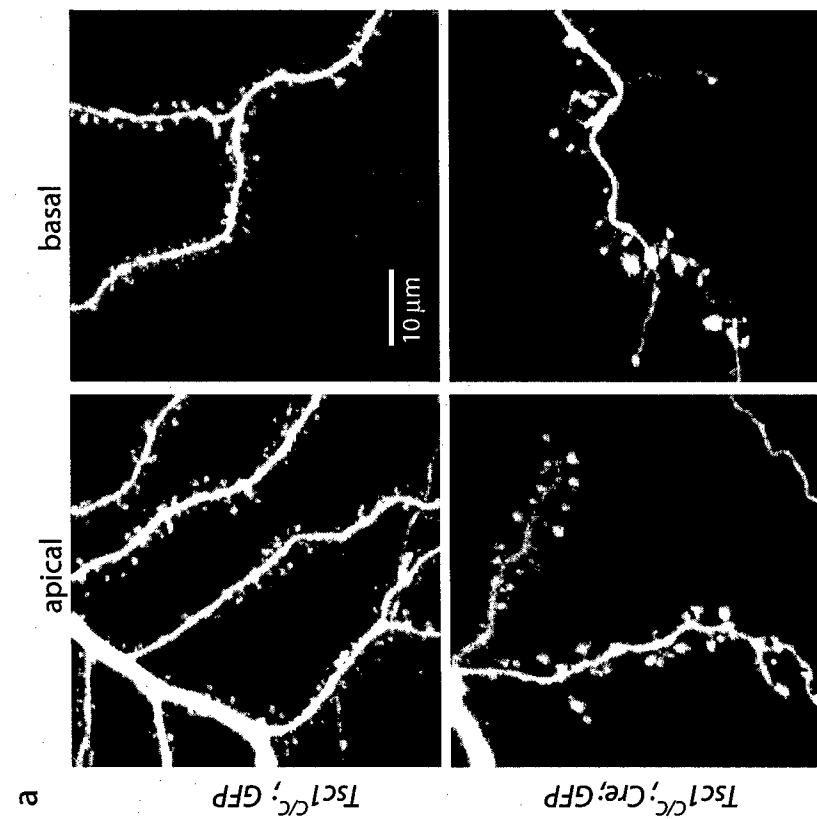


Figure 3

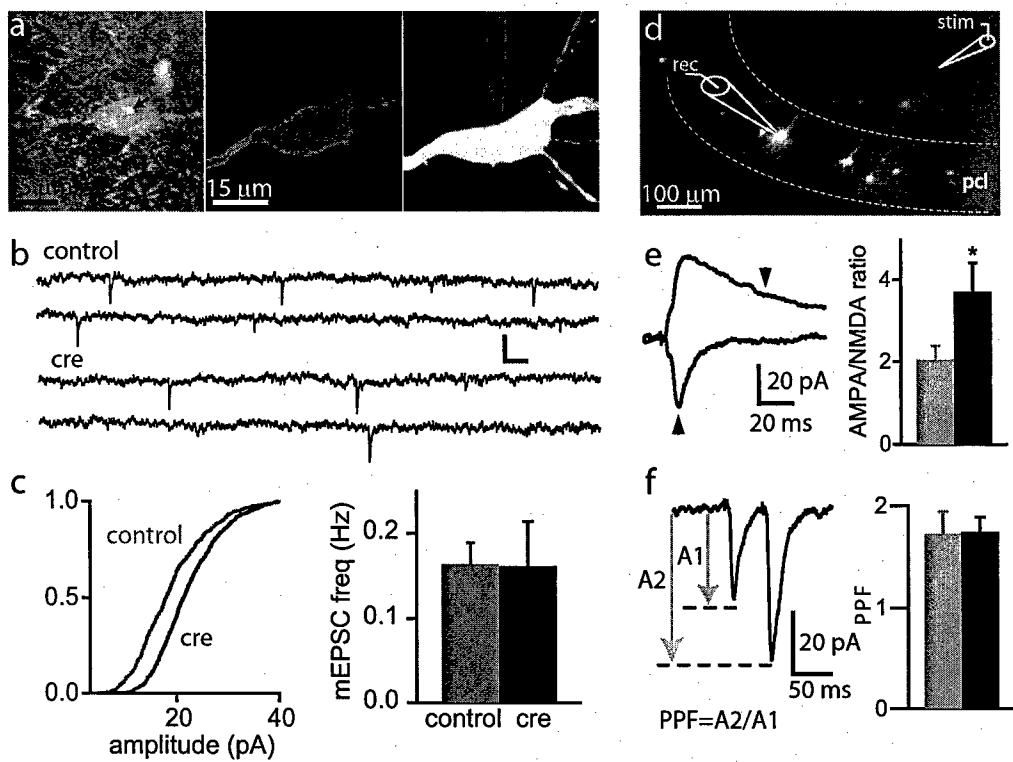


Figure 4

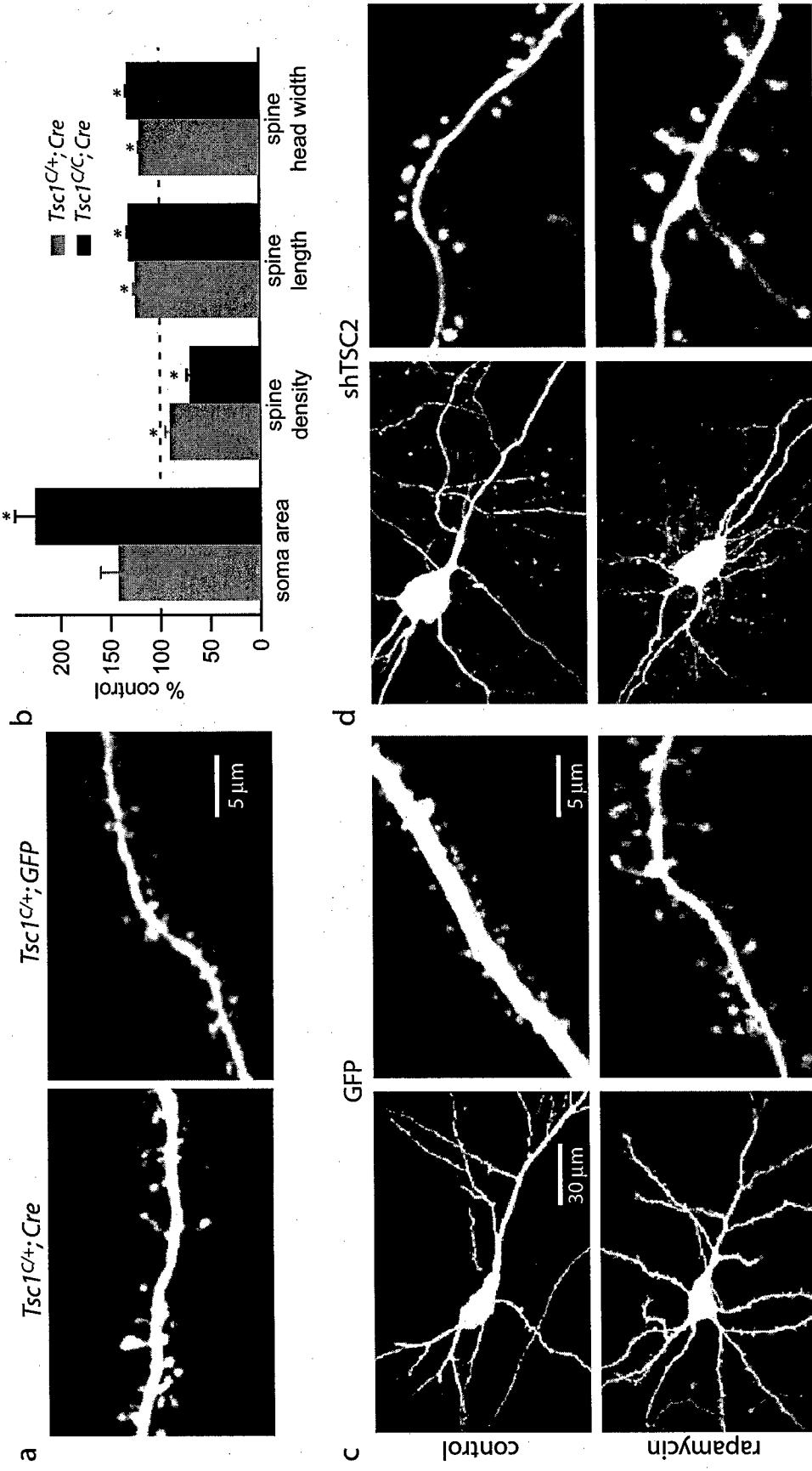


Figure 5

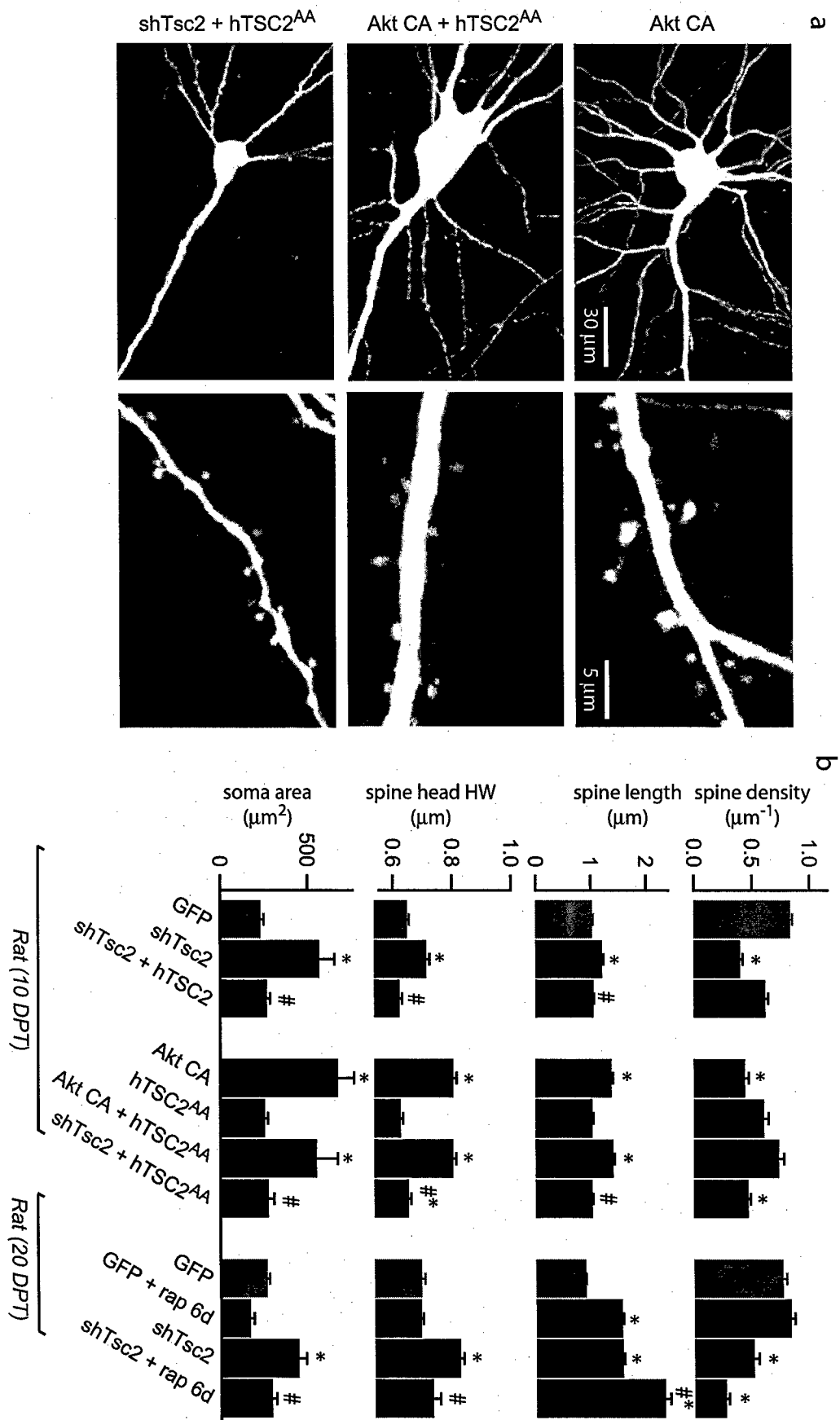
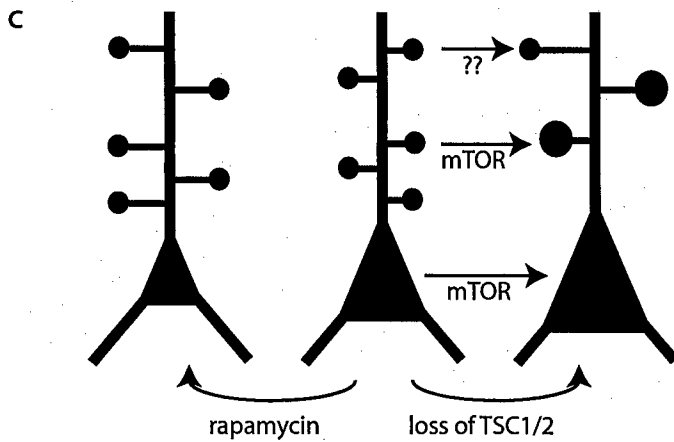
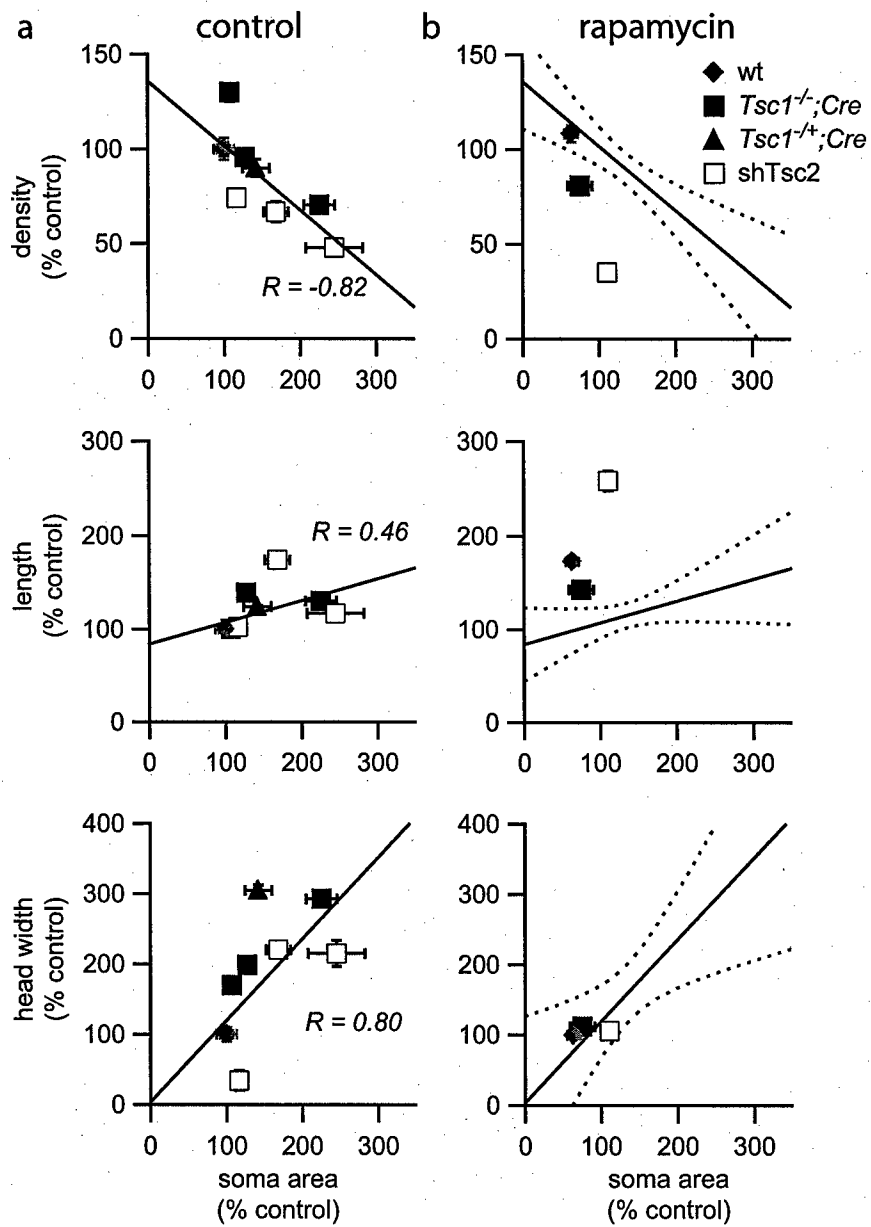
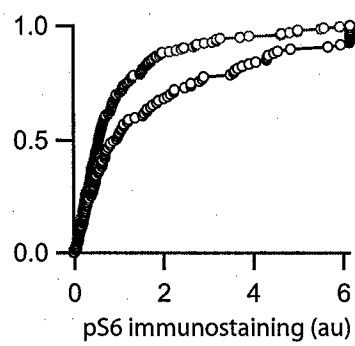
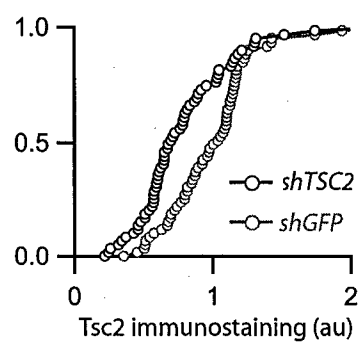


Figure 6



Supplemental Figure 1



GENOTYPE	CONDITION	DPT	N cells/spines	SOMA AREA μm^2	SPINES		
					DENSITY μm^{-1}	LENGTH μm	HEAD WIDTH μm
<i>Tsc1^{C/C}</i>	control	10	7 / 2577	240 ± 43 (12)	0.79 ± 0.02	0.90 ± 0.01	0.69 ± 0.01
	control	20	9 / 2441	280 ± 22 (20)	0.87 ± 0.03	0.99 ± 0.01	0.71 ± 0.01
	Cre	10	8 / 3338	287 ± 21	0.76 ± 0.03	1.26 ± 0.01	0.79 ± 0.01
	Cre	20	16 / 4344	583 ± 36 (31)	0.61 ± 0.03	1.29 ± 0.01	0.93 ± 0.01
	Cre, Tsc1	20	8 / 2960	275 ± 17	1.13 ± 0.04	0.99 ± 0.01	0.79 ± 0.01
	Cre, rapa	20 (6)	7 / 1938	228 ± 48	0.70 ± 0.04	1.42 ± 0.02	0.79 ± 0.01
<i>Tsc1^{C/+}</i>	control	20	4 / 1200	226 ± 37	0.85 ± 0.05	1.06 ± 0.01	0.72 ± 0.02
	Cre	20	11 / 2996	349 ± 45	0.77 ± 0.04	1.32 ± 0.01	0.84 ± 0.01
Rat	control	10	13 / 5023	303 ± 25	0.83 ± 0.02	1.03 ± 0.01	0.65 ± 0.01
	control	20	13 / 4262	360 ± 17	0.77 ± 0.03	0.91 ± 0.01	0.70 ± 0.01
	rapa	20	6 / 1702	170 ± 30	0.83 ± 0.03	1.57 ± 0.02	0.69 ± 0.01
	shTsc2	10	7 / 1715	705 ± 37 (17)	0.40 ± 0.02	1.21 ± 0.02	0.73 ± 0.01
	shTsc2, hTSC2	10	9 / 2682	340 ± 25	0.62 ± 0.02	1.06 ± 0.01	0.61 ± 0.01
	hTSC2 ^{AA}	10	5 / 1014	347 ± 25 (8)	0.61 ± 0.04	1.03 ± 0.02	0.67 ± 0.01
	shTsc2, hTSC2 ^{AA}	10	5 / 1824	419 ± 34	0.47 ± 0.02	1.03 ± 0.01	0.68 ± 0.01
	Akt CA	10	5 / 1052	932 ± 68 (18)	0.44 ± 0.03	1.38 ± 0.03	0.80 ± 0.01
	Akt CA, hTSC2 ^{AA}	10	5 / 1149	716 ± 66 (10)	0.73 ± 0.04	1.41 ± 0.03	0.80 ± 0.01
	shTsc2, rapa	10 (2)		270 ± 25 (5)			
<i>Rosa^{C/C}</i>	control	20	7 / 3522	195 ± 28	0.88 ± 0.03	1.04 ± 0.01	0.67 ± 0.01
	Cre	20	8 / 4187	205 ± 32	0.92 ± 0.04	1.02 ± 0.01	0.66 ± 0.01
	shTsc2, rapa	20 (6)	8 / 1163	420 ± 35	0.27 ± 0.03	2.34 ± 0.09	0.73 ± 0.02

Supplemental Table 1. Summary of analyzed data set. The columns are as follows:

Condition: The transfected plasmids are listed and 'rapa' indicates the presence of 100 nM rapamycin in the culture media.

DPT: The days post transfection (DPT) at which analysis was performed and, when applicable, in parenthesis in the same column is the number of days of application of rapamycin.

N: The number of cells and spines analyzed.

Morphological parameters: The average ± standard error of the mean are given. In a few cases images were acquired that were used only for analysis of soma area. In these cases, the total number of cells used in the soma analysis is given in parenthesis in the 'soma' column.